1999

Flange Bolt Failure Analysis

Tarun Goswami

FLANGE BOLT FAILURE ANALYSIS

Tarun Goswami

Materials and Processes Group (Dept. 178, MS 1), Cessna Aircraft Company
2617 South Hoover Road, Wichita, KS 67215
Department of Mechanical Engineering, Wichita State University, Wichita, KS 67260, USA

ABSTRACT

Failure cause investigation of flange bolts from the bi-axial shaft fatigue test rig was carried out and crack growth rates in combined bending and torsion conditions were determined. Flange bolts are used in gas turbine engines that are pre-torqued exerting bending and torsion fatigue situation arising from high centrifugal stresses. The fracture surface features were characteristic of bending fatigue (BF), where striations were observed, a distinct area within which conjoint bending and torsion fatigue (CBTF) features were documented, and a region between the BF and CBTF, a region of overloading (OL), where ductile dimples were observed. Striations dominated within BF and CBTF areas. The CBTF fracture comprised predominantly 80 percent or more of the total fracture surface area. However, as these two modes progress from opposite sides, the region between them experiences overloading and fails as a result. These features were documented for each case. Fatigue striations were counted for CBTF mode and crack growth rate as a function of crack length and crack length as a function of cumulative striations were presented. Since the failure occurred with the application of 60,000 minor cycles, cumulative striation counts were 1/5 of this life. The fatigue crack nucleation stage was affected since the part contained burr marks.

Key Words: Bending fatigue, conjoint bending torsion fatigue, overloading, striation, cleave, and ductile dimples.

INTRODUCTION

Gas turbine engines and their components such as flange joints operate under conditions where minor cycles, low amplitude high vibratory cycles, are superimposed on a major cycle. A major cycle

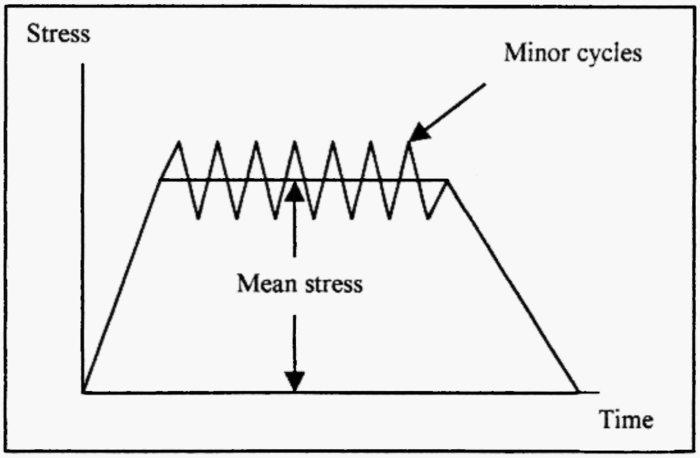

Fig. 1: Conjoint major-minor cycle interactions.

is a high amplitude, low frequency cycle. The minor cycles arise from flow fluctuations and other performance requirements. Therefore, conjoint actions of major-minor cycles, shown in Figure 1, have recently been gaining research attention /1-10/. Conjoint fatigue may have the potential to reduce the life of equipment drastically if favorable load and cycle ratios are imposed in service. Such failures are a result of high amplitude minor cycles and frequency, cycle ratio, at which they occur. Cycle ratio is a ratio of the number of minor cycles per major cycle. The effect of high amplitude ratio and high cycle ratio was investigated in the literature /1-10/, showing accelerated fatigue crack growth rates.

A different scenario is presented in this paper where a flange bolt was used under major-minor cycles under bending and torsion situation resulting from pre-torque which is applied to tighten the nut and torsion resulting from shaft rotation, respectively. The conjoint cycle comprised of 60 cycles/min or 300 cycles per major cycle. The bolts were removed from the bi-axial shaft fatigue rig after 200 major cycles and causes of failure were investigated. Therefore, in this paper causes of failure, fractography and appropriate data from the microscopic observations are presented.

MATERIAL

A superalloy, Nimonic 75A, was used as a fastener material. Conjoint fatigue studies were made on Ti-6Al-4V /1-3/, Inconel 718 /3,4/, GH 36 /5/ (iron-cobalt base material), low carbon steels /6-8/, and high strength steels /9,10/. Since these flange bolts are pre-torqued and the assembly experiences high centrifugal loads, therefore bending fatigue and bending torsion fatigue are two modes in which the damage takes place.

Details of solution heat treatment parameters, chemical composition and mechanical properties of Nimonic 75A have been tabulated in Tables 1-3. Bolts were made from a bar stock 16 mm in diameter. Microstructure of this bar stock is shown in Figure 2.

Table 1

Summary of chemical composition of Nimonic 75A

Cr	Si	Ti	Al	Fe	C	Mn	Ni	Cu
19.5	1	1	0.15	2.5	0.12	1	Bal	0.25

Table 2

Summary of heat treatment parameters used for Nimonic 75A

Solution Annealing	Solution heat treatment at 1975°F for 2 hours
	Aging at 1300°F for 16 hours.

Table 3

Summary of mechanical properties

Tensile strength	Percent elongation	Temperature	Strain rate
750 MPa	35	26°C	0.003

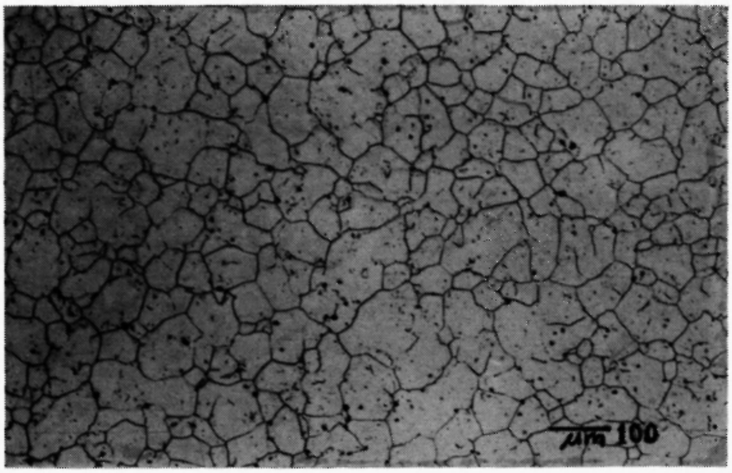

Fig. 2: Microstructure of Nimonic 75A (magnification 90X).

FRACTOGRAPHY

Minor cycle amplitudes are usually from 8 to 30 percent of the major cycle stress amplitudes /1-10/ commonly found in the literature. It is also shown /1-10/ that as the minor cycles are applied, accelerated fatigue crack growth rates occur. Figure 1 shows a typical cycle that has the segments of ground-air-ground cycle for an aircraft engine or power equipment, where peak loads are achieved in terms of no-load to a peak-load situation. Figure 1 can be used to show a component of either bending (major cycle) and torsion (minor cycles) or vice-versa. Since the BF and CBTF features are the subject of this paper, BF and CBTF fractography is discussed in more detail in the following sections.

Figure 3 shows the fracture surface of the bolt. The BF area nucleated from the root of a screw

(a)

(b)

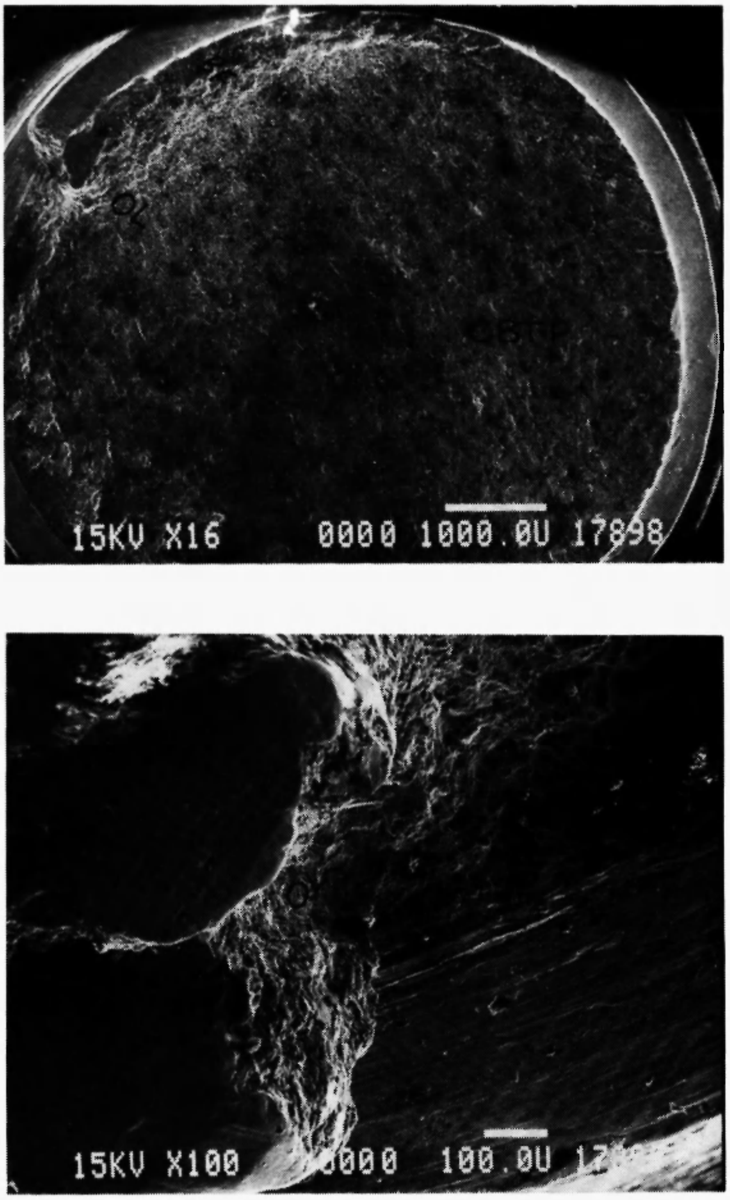

Fig. 3: (a) Montage of fracture surface; (b) Failure origin.

thread. Three divisions made on the fracture surface show BF, Fig. 3(a), overloading (OL), Fig. 3 (b) and CBTF, Fig. 3 (a), on the montage of the fracture (Fig. 3 (a,b)). Each fracture surface from a set of six failed bolts had similar characteristics. They were:

Bending Fatigue:

Within this area striations were documented. Fracture surface area exhibiting BF features ranged from less than 10 percent of the total area. Figure 4 shows the striations made in the BF area; the arrow marked in this figure shows the direction of crack propagation. Kink bands were observed indicative of sudden increase in stress intensity factor. As a result of this feature crack path also turned in the direction of the band. Since the cycle used was conjoint bending and torsion involving major-minor cycles, application of each major cycle produced features such as kink bands and crack path changes.

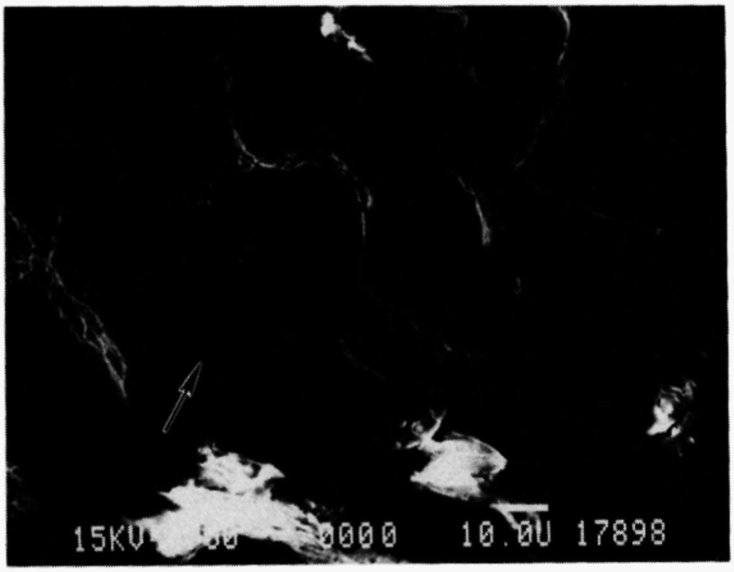

Fig. 4: Kink bands.

Overloading:

The striations, as shown in photomicrograph Fig. 4, ran from the left-hand side to right-hand side in the upward direction. Figure 3 (b) shows the area where the presence of micro-voids was documented, Fig. 5. Further right in this figure ductile dimples occur. Figure 5 shows a typical OL area and associated fracture features. Within this area micro-voids are clearly seen that were made due to the overloading nature of the loads. Macro-voids seen are a result of pulling of strengthening phases of carbide particles.

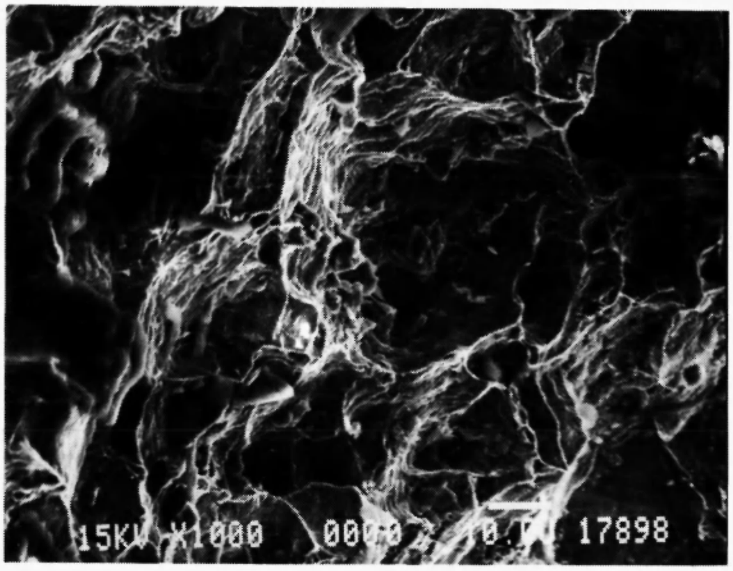

Fig. 5: Ductile dimples indicating OL mode.

Combined Bending and Torsion Fatigue

At the area close to the right-hand side of the fracture surface, Fig. 3, cleavage type features were observed. Since cleavage occurs at the low and high range of stress intensity factor, it does not occur in superalloys having tensile strength of 750 MPa or above. However, since this material is within that boundary in terms of tensile strength, some cleavage like features were found at an area close to RHS of the fracture surface. Kink bands discussed in BF were also observed in this area. Since the applied waveform was a mixture of high-low amplitude cycles, pitching of fracture plane was observed at several points. This pitching effect in the fracture surface may have been caused by the mean stresses arising from major cycles. Multiple cracks were generated in the case of CBTF, which had independent paths and directions and affected the CBTF crack growth patterns. Crack curvatures were different in different directions. Such a behavior presents complexities in the treatment and use of data for crack growth determination. However, this behavior was observed away from the path of the crack upward in the direction of the arrow shown in Figure 4.

Figure 6 shows striations and their progression in the CBTF area. The CBTF area was considerably larger than the BF and OL areas and therefore it was possible to identify striations ranging in different sizes in Figures 6 and 7. Voids were documented on the fracture surface together with striations, Figures 6 and 7, indicative of particle pulling and some overloading.

Since striations were found at most of the fractured area from the crack origin, in this case from the root of a screw thread, BF and CBTF modes contributed to the failure of the flange bolts. Various

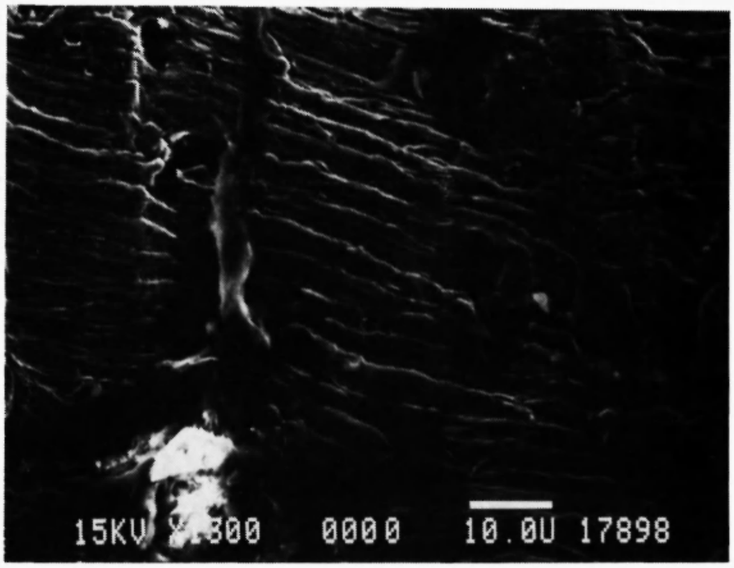

Fig. 6: Fatigue striations and cleavage.

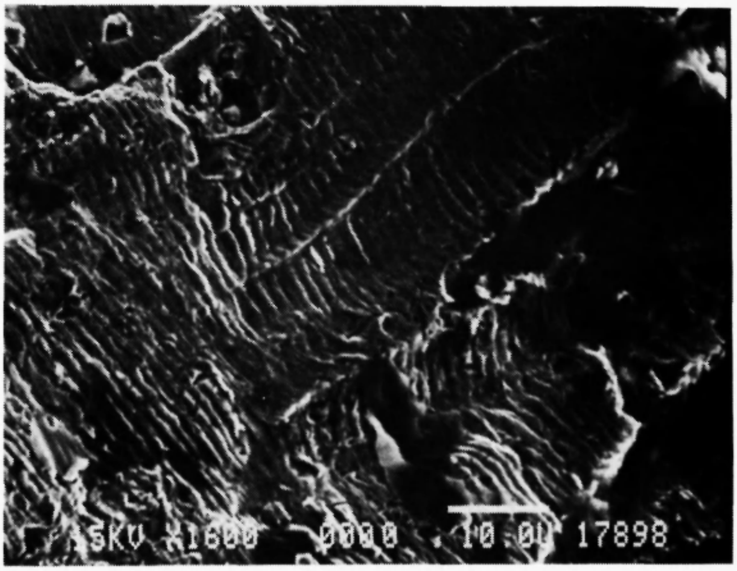

Fig. 7: Fatigue striations and dimples.

measurements made for the striation counts can be found in Figures 8 and 9. These figures show crack growth rate as a function of crack length and crack lengths as a function of striations, respectively. Figure 8 shows that the width of the striations increases from the LH side in the CBTF area towards a point between the CBTF and OL area. Further away from the CBTF point of origin, the width of

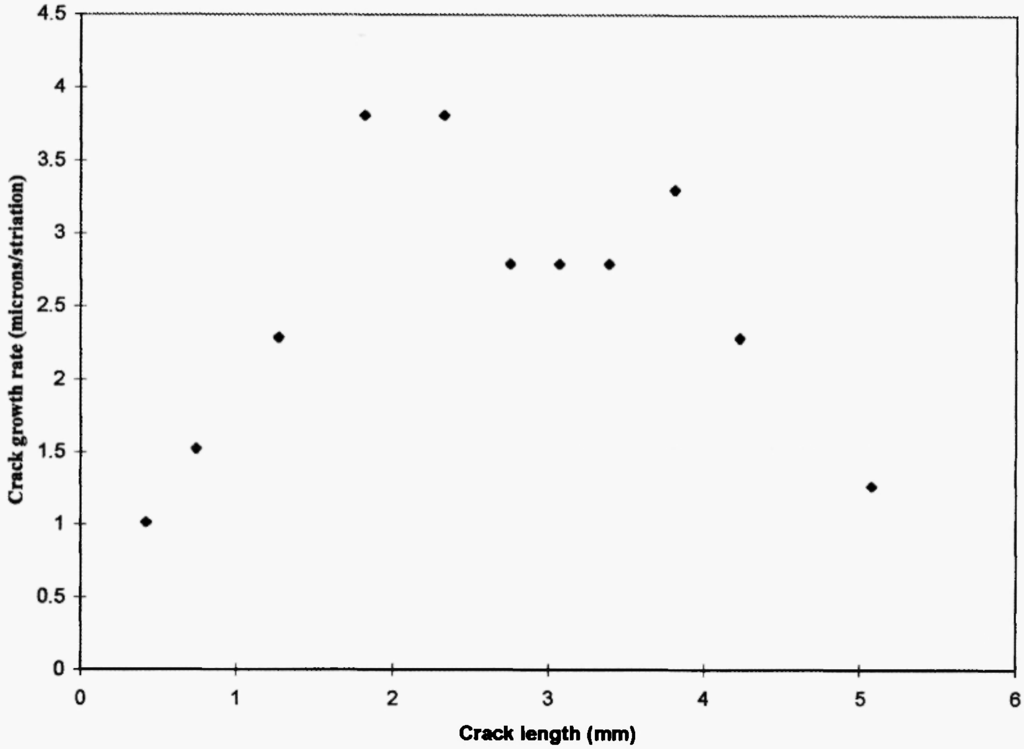

Fig. 8: Crack growth rate as a function of crack length.

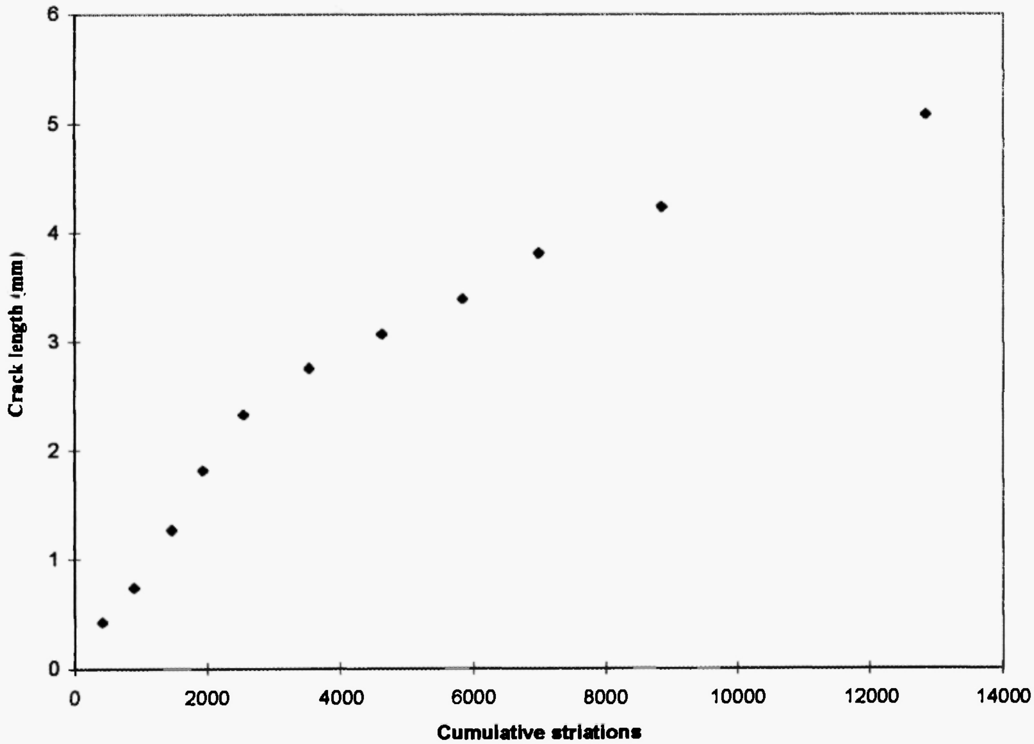

Fig. 9: Crack length as a function of cumulative striations.

striations does not change considerably, resulting in low crack growth rates. Figure 9 shows these trends and two linear phases between the crack length and the cumulative number of striations. The data generated in terms of crack length, crack growth rate and cumulative striations are presented in Table 4. A modified Bates equation /11/ can be applied to this data to determine crack growth rate, and mode I stress intensity factor range (ΔK) relations. Some of the fracture surface features, for example, cleavage, kink band formation, block striations were also reported by other workers /1-10/ in a range of materials.

Table 4

Crack growth data from the striation counts

Crack length (mm)	Crack growth rate (microns/striation)	Cumulative striations
0.423	1.016	417
0.740	1.524	903
1.27	2.286	1459
1.82	3.81	1937
2.32	3.81	2548
2.75	2.794	3533
3.06	2.794	4631
3.38	2.794	5843
3.81	3.302	6997
4.233	2.286	8849
5.08	1.27	12849

It is possible to argue that conjoint CBTF crack growth and failure may have been controlled primarily by plastic strains. Since the flange bolts exhibited poor elastic modulus, it may have contributed to a low CBTF resistance in the presence of burr marks and stress concentrations arising from screw threads. Therefore, major-minor cycles used in this study and geometrical stress raisers (screw threads) may have amplified the range of stress intensity factors that generated increased crack tip interaction zone, thereby reducing the tendency of a crack to follow through the crystallographic paths. Kink bands were a result of higher amplitude deformation and caused pitching of the crack planes. Micro-voids within the fatigue striations on the fractographs are indicative of some degree of overloading.

Cumulative striations were seen for nearly 13,000 striations and the failure of the flange joint, which contained six bolts, occurred after application of 60,000 minor cycles. Crack propagation mode in the failed flange bolts was dominated by CBTF. However, a component of BF is also present in the fractograph, which was not accounted for. Given the major damage fraction from CBTF, which comprised 1/5 of the life, the crack nucleation phase was difficult to estimate given that burr marks were evident on the threaded area of the bolt.

CONCLUSIONS

1. The BF features were dominated by striations. Some kink bands were also observed.
2. The OL features were ductile dimples created by micro-void nucleation and growth.
3. The CBTF features were cleavage type but mainly dominated by striations. Kink bands and multiple crack paths were documented. Pitching of fracture surface also occurred.
4. The CBTF contributed nearly 80 percent of the crack growth life; therefore it is a dominating failure mechanism of flange bolts.
5. The failure occurred from the root of a screw thread in the CBTF mode.

REFERENCES

1. B.E. Powell, T.V. Duggan and R. Jeal, *Int. J. Fatigue*, **4**, 4 (1982).
2. B.E. Powell and T.V. Duggan, *Int. J. Fatigue*, 9(4), 195 (1987).
3. J.Y. Guedou and J.M. Rongvaux, ASTM STP 942, 1987 938.
4. T. Goswami and A.K. Prasad, Unpublished work at Gas Turbine Research Establishment.
5. J. Quyang, Z. Wang, D. Song and M. Yan, ASTM STP 1987 961.
6. T. Tanaka and S. Denoh, *Bull. Japan. Soc. Mech. Eng.*, **2**(4), 77 (1968).
7. T. Tanaka and S. Denoh, *Bull. Japan. Soc. Mech. Eng.*, **12**(54), 1309 (1969).
8. T. Tanaka and S. Denoh, *Bull. Japan. Soc. Mech. Eng.*, **14**(77), 1139 (1979).
9. G.Z. Zaitsev and R.M. Faradzhov, The fatigue limit of steels under loads of differing frequencies, *Metallovedenie I Obrabotka Metallov*, **2**, 44 (1970).
10. N. Mukhukov, A. Romanov and M. Gardenin, *Fatigue of Eng. Mater. Struct.*, **1**, 281 (1979).
11. R.C. Bates and W.G. Clark Jr., *Quarterly Trans. ASM*, **62** (2), 1969.